Biopolymer Mimicry with Polymeric Wormlike Micelles: Molecular Weight Scaled Flexibility, Locked-in Curvature, and Coexisting Microphases*

PAUL DALHAIMER, HARRY BERMUDEZ, DENNIS E. DISCHER

Department of Chemical and Biomolecular Engineering, University of Pennsylvania, Philadelphia, Pennsylvania 19104

Received 10 June 2003; revised 20 August 2003; accepted 22 August 2003

ABSTRACT: Giant and stable wormlike micelles formed in water from a series of poly(ethylene oxide) (PEO)-based diblock copolymer amphiphiles mimicked the flexibility of various cytoskeletal filaments. The worm diameter (d) was found by cryo-transmission electron microscopy to scale with the length of the hydrophobic chain (N_h) of the copolymer as $d \sim N_h^{0.61}$. By fluorescence video imaging of worm dynamics, we also showed that the persistence length (l_P) of wormlike micelles scaled as $l_P \sim d^{2.8}$, consistent with a fluid aggregate ($\sim d^3$) rather than a solid rod ($\sim d^4$). By polymerizing the unsaturated bonds of assembled copolymers, fluid worms were converted to solid-core worms, extending the bending rigidity from that of intermediate filament biopolymers to actin filaments and, in principle, microtubules. Through partial crosslinking, polymerized worms further locked in spontaneous curvature at a novel fluid-to-solid percolation point. The dynamics of distinct, branched conformations were also imaged for recently discovered Y-junctioned wormlike micelles composed of diblocks of high molecular weight (>10–15 kg/mol). Finally, block copolymers of hydrophilic weight fraction close to the transition between a vesicle- and worm-former assembled into both structures, allowing encapsulation of wormlike micelles in giant vesicles reminiscent of cytoskeletal filaments enclosed within cells. © 2003 Wiley Periodicals, Inc. J Polym Sci Part B: Polym Phys 42: 168–176, 2004

Keywords: worm micelle; assemblies; diblock copolymer; amphiphiles

INTRODUCTION

Mimicry of cell and biomolecular structures via purely synthetic chemistries is potentially of wide interest. With proper control over structure(s) and mixtures, there is hope of emulating functions that might range from muscle contraction for device actuation to artificial viruses for drug delivery. The lipid bilayer is already one successfully mimicked cell biological structure with a recent strictly synthetic approach making use of moderate-molecular-weight diblock copolymers (several kilograms per mole) composed of poly(ethylene oxide)-polybutadiene (PEO-PBD) and/or poly(ethylene oxide)-polyethylethylene (PEO-PEE).[1,2] These amphiphilic copolymers self-assemble in water to give highly stable vesicles. Many related systems and copolymers have been developed and observed in recent years.[3–5] Both PEO-PBD (abbreviated OB) and PEO-PEE (abbreviated OE) of higher PEO weight fraction than those used to make vesicles have also formed wormlike micelles[6] that are many micrometers long and highly stable in flow[7] but only ~10 nm in diameter.[6] Interestingly, despite their simplicity, the

*Contribution from the March 2003 Meeting of the American Physical Society—Division of Polymer Physics, Austin, TX

Correspondence to: D. E. Discher (E-mail: discher@seas.upenn.edu)

Journal of Polymer Science: Part B: Polymer Physics, Vol. 42, 168–176 (2004)

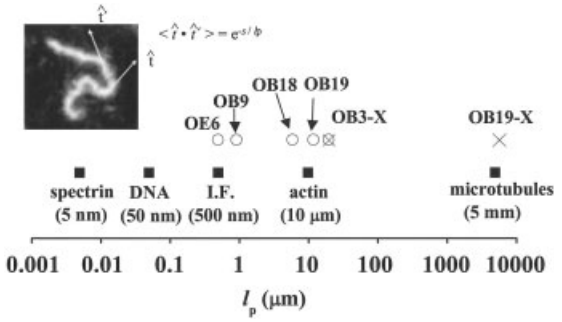

Figure 1. Persistence lengths of OB and OE wormlike micelles plus selected blends (details in Table 1) as compared to ubiquitously expressed biopolymers (open squares). Inset shows formula for calculating l_P for worms stiffer than OB9 through vectors tangent to the worm backbone separated by distance, s[11]. l_P for worms with flexibility equal to or greater than OB9 is calculated with $\langle R^2 \rangle = 2l_P L[1 - l_P/L(1 - e^{-L/l_P})]$, where R is the end-to-end distance of the worm, and L is the contour length.[11] OB class worms can be pristine (open circles) or fully crosslinked through polymerization (circles with X). OB diblocks can be polymerized (X), and OE diblocks can be added to dilute the crosslinks and decrease worm stiffness. OB19 worms have diameters that are ~2.5 times larger than OB3 worms. Therefore, from beam theory, fully crosslinked OB19 worms would be 50 times stiffer $(d_{OB19}/d_{OB3})^4$ than a fully crosslinked OB3 worm ($l_P \sim 115$ μm); although not easily measured, this would give $l_P \sim 6$ mm (X), which rivals the stiffness of a microtubule. Fully crosslinked OB worms are indicated by OB#-X.

worms have bending rigidities similar to those of complex cytoskeletal biopolymers ranging from intermediate filaments[8] to F-actin[9,10] (Fig. 1). Free-radical polymerization of PBD in the hydrophobic cores of PEO-PBD and PEO-PEE blended worms provided one means of control over flexibility.[7] We extend and generalize such efforts here with a considerably broadened class of copolymers and novel microstructures.

Giant wormlike micelles[6,12,13] of EO_{55}-BD_{45} have already been readily labeled by hydrophobic fluorophores thus allowing fluorescence imaging of dynamics at the single-molecule level.[7] Our focus here is on the diameter-dependent flexibility and microphases of related OB- and OE-type copolymers listed in Table 1. The copolymers varied in molecular weight by an order of magnitude with those of the PEO weight fraction $w_{EO} < 0.45$ forming mainly bilayer vesicles and those of $0.45 < w_{EO} < 0.55$ forming mainly wormlike micelles.[15,16] The hydrophobic core diameter (d) was determined from cryo-transmission electron microscopy (TEM) imaging of individual worms and increased systematically with copolymer molecular weight, broadening the properties of these structures.

A persistence length of ~0.5 μm for both OE6 and pristine OB3 worms was calculated in a first report[7] on worm dynamics by fluorescence techniques also used here. The stability of the giant worms was remarkably high with a self-association energy $\alpha \geq 26\ k_BT$.[7] Consistent with such stability, copolymer worms of contour length $L > 100$ μm have been observed and, typically, $\langle L \rangle \sim 10$ μm.[7,12] These initial characterizations provided a starting point for mimicry of biopolymers that have diameters, persistence lengths, and contour lengths even greater than the aforementioned values.

EXPERIMENTAL

Diblock copolymers were prepared with a two-step anionic polymerization procedure.[17] Copoly-

Table 1. Structural Details of OE and OB Diblock Copolymers. Diameters Denoted by (*) Were Determined with a Best Fit of Referenced and Measured Data. OB18 and OB19 Diameters Were Directly Measured from Cryo-TEM Images. (†) Denotes a Y-Junction Former

Designated Name	Polymer Formula	M_n (kg/mol)	w_{EO}	Worm d (nm)
OE2	EO_{44}-EE_{29}	3.6	0.54	10.8*
OE6	EO_{46}-EE_{37}	4.1	0.48	12.5*
OE7	EO_{40}-EE_{37}	3.9	0.45	11.4[14]
OB3	EO_{55}-BD_{45}	4.9	0.51	14.2[6]
OB9	EO_{50}-BD_{54}	5.2	0.43	15.7*
OB18	EO_{80}-BD_{125}	10.4	0.35	27
—	EO_{105}-BD_{170}	14†	0.34	34[15]
OB19	EO_{150}-BD_{250}	20†	0.33	39

mers were dissolved in chloroform and dried on glass to form a film that was hydrated with water at 50–60 °C. A hydrophobic fluorophore dye (PKH26; Sigma) was used to visualize the worms in a pseudo-two-dimensional (2D) chamber formed between two coverslips.[7] Worms were imaged with an Olympus IX71 inverted fluorescence microscope with a 60× objective and a Cascade charged coupling device camera. Cryo-TEM samples were prepared and analyzed as described elsewhere.[6,18]

RESULTS AND DISCUSSION

There are at least two ways to explore augmentation of the bending rigidity of wormlike micelles given this chemistry: (1) chemically crosslink the BD blocks in the worm core to create a solid wormlike micelle;[2,6,7] and/or (2) increase the diameter of the worm by assembling the worm from larger copolymers. The latter can in principle have its subtleties, but free-radical crosslinking within OB3 worms has already been shown to increase the worm-persistence length by more than 100-fold from $l_P = 0.5$ μm to a crosslinked value, $l_{PX} \sim 100$ μm.[7,12] Moreover, to interpolate both within this range of rigidities and from fluid-to-solid states, a PEO-PEE analogue of OB3 (OE6) can be blended into the worm in varying concentrations before free-radical polymerization of the PBD double bonds.[7] Although such blending and crosslinking is increasingly understood, the subtlety in controlling rigidity with worm diameter stems from the hypothesis that molecules in a fluid worm will rearrange and significantly relax any curvature stress.[15] We explore both methods of worm stiffening subsequently. We focus specifically on scaling of l_P with d as well as worm branching and spontaneous curvature effects in crosslinking. Cytoskeletal mimics are an inspiration if not an ultimate goal.

Worm Flexibility versus Cytoskeletal Filaments

As compared with cytoskeletal filament rigidities, Figure 1 summarizes the preceding crosslinking result and adds to it the measured persistence lengths for giant wormlike micelles formed from a broader representative subset of copolymers in Table 1. As the inset in Figure 1 illustrates, we obtained l_P from a tangent–tangent correlation function for OB18 and OB19 worms and an integrated version of the tangent–tangent correlation

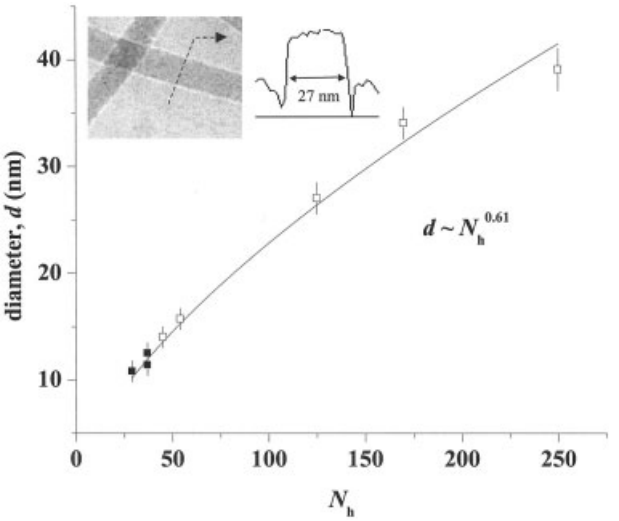

Figure 2. Scaling relationship of wormlike micelle d as a function of the number of N_h's in OE (closed squares) and OB (open squares) class copolymers in Table 1. Diameters were measured from cryo-TEM images of the worms. The inset cryo-TEM image shows an OB18 wormlike micelle and the cross-sectional intensity profile used to estimate its diameter, $d = 27$ nm.

function involving fluctuations in the end-to-end length for all other, more flexible worms.[11] Persistence lengths for pristine PEO-PBD and PEO-PEE worms are indicated by labeled open circles; crosslinked PEO-PBD worms are marked with crossed circles, and the name of the copolymer comprising the worm is followed by an X (e.g., OB3-X is fully crosslinked OB3). By combining techniques (1) and (2) above, OB worms of large diameter (up to $d = 39$ nm; Table 1) can be fully crosslinked to form almost inflexible solid cylinders (OB19-X) with a persistence length approaching that of a microtubule.[9] The copolymers listed in Table 1 thus span bending rigidities of ubiquitously expressed biopolymers that ranged from intermediate filaments to microtubules.

Measurements of d from cryo-TEM images showed a systematic dependence on the length of the hydrophobic chain (N_h), which has also been found for membranes.[18] By fitting a power law to the referenced and measured data in Table 1, we find the curve shown in Figure 2, where the diameter of the worms fits best to $d = 1.38 N_h^{0.61}$. A fully stretched polymer of N_h groups would theoretically assemble into an object with diameter, $d \sim N_h^1$, whereas ideal random coils, such as in a melt, would give an object with $d \sim N_h^{0.5}$. The copolymers examined here were in the strong segregation limit (SSL) where interfacial tension (γ)

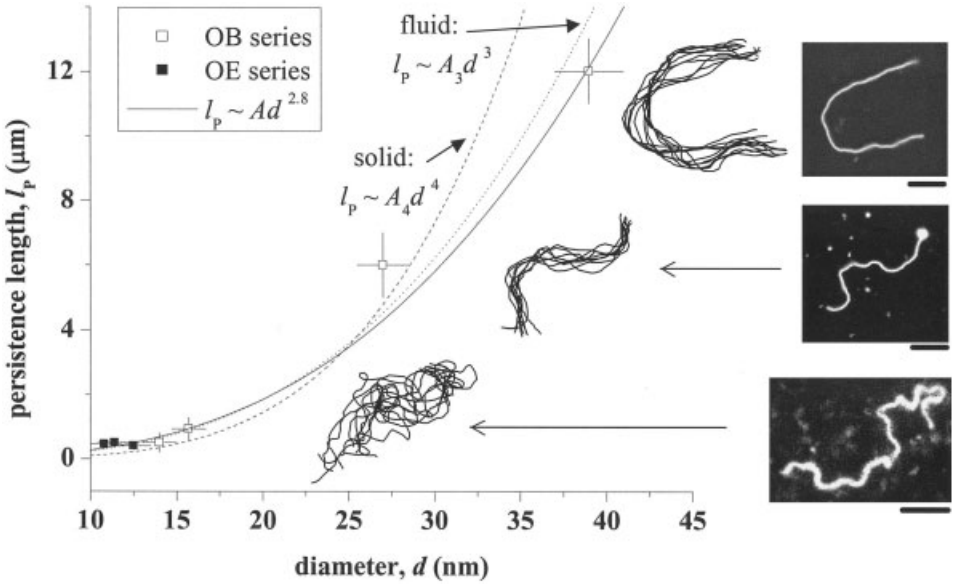

Figure 3. Stiffness of l_P's as a function of hydrophobic core d. Diameters were calculated from cryo-TEM images, and persistence lengths were calculated from fluorescence video microscopy for seven different worm-forming diblock copolymers listed in Table 1. Inset images show fluorescence snapshots of three different pristine wormlike micelles of varying stiffness freely diffusing in a pseudo-2D chamber along with backbone traces taken every ~0.5 s. When fit by power laws, the bending rigidities of these worms scale as $l_P \sim d^{2.8}$, which is closer to the scaling relationship for a fluid than a solid cylinder ($A = 0.0004$, $A_3 = 0.00023$, $A_4 = 9 \times 10^{-6}$). Note that the l_P value for OB19 represents only wormlike micelles and not OB19 Y-junction structures, which are discussed subsequently (scale bars are 5 μm).

balanced chain entropy so that $d \sim N_h^{0.67}$ is expected.[18–20] The scaling exponent obtained here of 0.61 is thus slightly closer to the SSL expectations than the scaling found for membranes assembled from a subset of the same copolymers in Table 1. Moreover, the radius of gyration (R_g) can be calculated with $R_g = b\,(N_h/6)$, where $b = 0.54$ nm has been experimentally determined for the PEO-PEE copolymers.[21] For OE7, for example, $R_g = 1.3$ nm, which indicates that the copolymer is stretched about four- to fivefold as compared to the worm radices, $d/2$ (Table 1). This result is fully consistent with strong lateral squeezing of chain configurations by interfacial tension that extends the chain into the core and thus forms the basis for SSL theory. Thus, although scaling of d with N_h alone ($d \sim N_h^{0.61}$) is less convincing of SSL versus a simpler melt ($d \sim N_h^{0.5}$), the strong stretching is indicative of SSL. Furthermore, the mean end-to-end length (R) of a given polymer is slightly larger than its R_g (in fact, $R/R_g \sim \sqrt{6}$[22]), but R is still much smaller than $d/2$ and implied than an oriented chain with one end pinned at the interface by PEO still being laterally squeezed and extended.

Given the wide range of core d's for the worms in Table 1, we were also able to experimentally determine the scaling relation for the worm-persistence length (l_P). Dimensional analysis informed us that a fluid cylinder whose rigidity is dominated by γ has a persistence length that scales with core diameter in the form $l_P = \phi\gamma d^3/k_BT$, where ϕ is a constant.[7] On the basis of extensive measurements of membrane elasticity, γ is already known to be a single constant for the OB and OE series of copolymers examined here.[18] Conversely, a solid rod or cylinder, also of d, follows the classical beam theory scaling of $l_P \sim d^4$,[23] where the energy scale for a beam is set by an elastic constant (E) for the core rather than by γ. Figure 3 illustrates the calculated persistence lengths of worms of varying hydrophobic core diameters with fluorescence snapshots and backbone traces of three worms representative of small, medium, and large d values. The best fit of the data gives a scaling exponent of 2.8. Despite chain entanglement in the core, which could effectively solidify it, the scaling result here more closely follows the cubic scaling behavior of classical fluid assemblies of lipid-size amphiphiles rather than solid-core cylinders or beams. With this exponent and $\gamma = 25$ pN/nm, we find $\phi = 1/20$

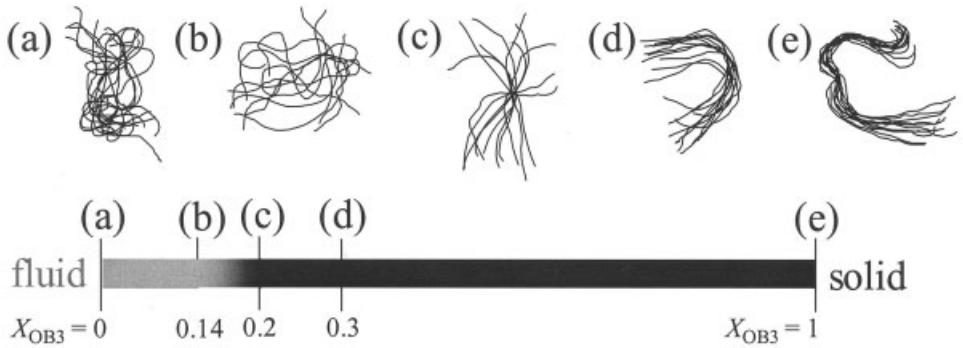

Figure 4. Backbone traces of chemically crosslinked OB3/OE6-blended wormlike micelles showing the spontaneous curvature of worms just above and below the percolation point ($X_{OB3} \sim 0.15–0.2$). Each trace was taken every ~0.3 s.

in $l_P = \phi\gamma d^{2.8}/k_BT$. Remarkably, this result is similar to lipid assemblies with $\phi = 1/30$ characteristic of semicoupled monolayers.[24]

Crosslinking Percolation and Spontaneous Curvature

As mentioned previously, crosslinked blends of PEO-PBD and PEO-PEE copolymers form worms that span bending rigidities between the fluid PEO-PEE worm (or pristine PEO-PBD worm) and the fully crosslinked, solid PEO-PBD worm.[7] A percolation in worm stiffness has already been seen at a critical PEO-PBD molar fraction of $X_{BD} = 0.15–0.2$ for blended worms of OB3/OE6.[7] In addition to a linear increase in stiffness beyond $X_{BD} = 0.2$ for OB3/OE6 worms, spontaneous curvature was locked-in above the percolation point as demonstrated in the backbone traces of Figure 4. Below the percolation point, worms have a radius of curvature that vanishes in thermal averaging [Fig. 4(a)]. However, when the amount of crosslinked PEO-PBD is increased through the percolation molar fraction [Fig. 4(b,c)], the increasingly solidified worm backbone fluctuates about a nonzero curvature conformation until it finally exhibits only a rigid-body rotation about an easily identifiable, spontaneously curved conformation [Fig. 4(d,e)].

As a simple model of stiffness modulation, we generalize the central-force percolation model applied to membranes by Discher et al.,[2] which assumes six neighbors for each butadiene bond in a $D = 2$ closed-packed triangular network geometry. Here, we consider a $D = 3$ extension of the previous model where each butadiene bond has $Z = 12$ coordinated neighbors because of hexagonal close packing in offset triangular networks. In both cases, there is a quasi-linear decrease in the elastic constants down to the critical molar fraction $X_C = p_C/N_C$, where p_C is the rigidity percolation limit derived from mean field arguments, and N_C introduces system size as the number of close-packed layers spanning the core diameter.[25] For X above X_C, the membrane is solidlike, and for X below X_C, the membrane is fluidlike; these predictions have been confirmed by fluorescence photobleaching experiments reported elsewhere.[26] For a triangular network $p_C = 2/3$, and in general for a D-dimensional central-force network, $p_C = 2D/Z$.[27] Solving these equations with the measured $X_C = 0.15$ for both geometric cases ($D = 3$, $Z = 12$), we arrived at $N_C = 3–5$ across the worm diameter.

To provide a more explicit picture of the preceding result for fully crosslinked OB3 worms, we considered the hydrophobic core upon chemical fixation to be a network of springs (newly formed crosslinks), a large fraction of which must act parallel to the worm's stiffened backbone. For a force $F = k_{eff}\Delta L$ applied parallel to the backbone, ΔL is the extension of the worm's contour length, and k_{eff} is the cumulative spring constant of N_X newly formed interchain crosslinks across any cross section such that $k_{eff} = N_X \cdot k_X$. Because $k_{eff} = AE/L$, where A is the cross-sectional area of the hydrophobic core (~160 nm^2), E is the Young's modulus of the worm, and L^2 is the interfacial area of a butadiene polymer (~1 nm^2),[28] we need only to obtain E from $l_{PX} = EI/k_BT$, as calculated elsewhere to be $E = 400$ MPa.[7,9] Therefore, $k_{eff} = 64$ N/m, which is ~1000-fold the tension at an air–water interface. To calculate k_X, knowing k_{eff}, we have to estimate N_X, which is also recognized

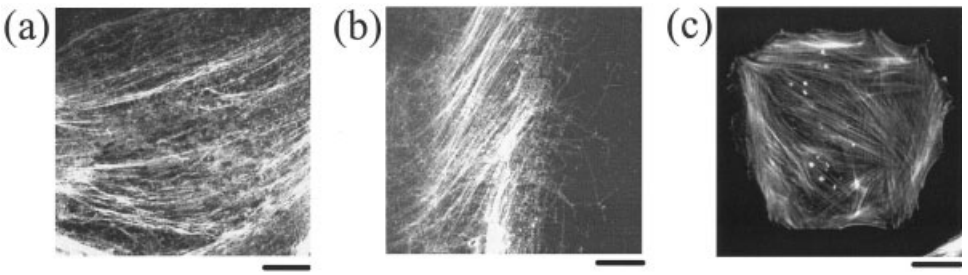

Figure 5. Concentrated regions of wormlike micelles resembling actin cytoskeletons. (a and b) Snapshots of sparse wormlike micelle networks formed due to capillary forces between the glass slide and coverslip that concentrate the worms into concentrated domains. In (a) and (b), nematic domains contrast with isotropic regions that are reminiscent of a cell cytoskeleton (c) with Rhodamine-labeled F-actin. Worms are labeled with a hydrophobic dye (scale bars are 20 μm).

as the number of crosslinks one would sever if the worm were cut perpendicular to its backbone. On each exposed face of such a cross section, there are ~45 OB3 copolymers where each copolymer contributes $\sim 0.5N_C(Z/2)$ crosslinks; hence, $N_X \approx 0.5N_C(Z/2) \cdot 45 \approx 540$ and $k_X = 64/540 = 0.12$ N/m. Therefore, to have a worm with a bending rigidity $l_{PX} \approx 115$ μm, one needs ~540 crosslinks approximately parallel to the worm axis.

Emulating Cytoskeletal Networks and Branched Systems

Because single wormlike micelles emulate the stability and flexibility of several cytoskeletal biopolymers, it follows that sparse networks of wormlike micelles might also mimic the collective features of locally concentrated cytoskeletal structures. Figure 5(a,b) shows two snapshots of OB3 wormlike micelle networks drawn out by simple capillary forces between a glass slide and coverslip. Both images show the great length of the worms. The results also highlight the nematic order achievable in single-domain networks, which appear similar in organization to actin cytoskeletons of typical tissue cells [Fig. 5(c)].

As the aforementioned spread cell suggests, a current and future challenge in synthetic cell design is to encapsulate filamentous structures such as wormlike micelles [e.g., Fig. 5(a,b) inside of a stable bilayer vesicle]. The goal is to emulate both the elasticity of a cell's scaffolding as well as the isolation of the structure from the external environment, eventually allowing for regulated assembly of synthetic structures. Because copolymers listed in Table 1 have a w_{EO} close to the vesicle/worm transition, they tend to form both assemblies upon film hydration. Figure 6 depicts fluorescence snapshots of an OE7 worm encapsulated in an OE7 bilayer vesicle along with schematic overlays of the system. The backbone of the fluctuating worm tends to define a thermally averaged ring against the unflexing vesicle bilayer—similar to observations of actin filaments encapsulated in lipid vesicles.[29] The lack of attraction or adhesion between vesicle and worm is

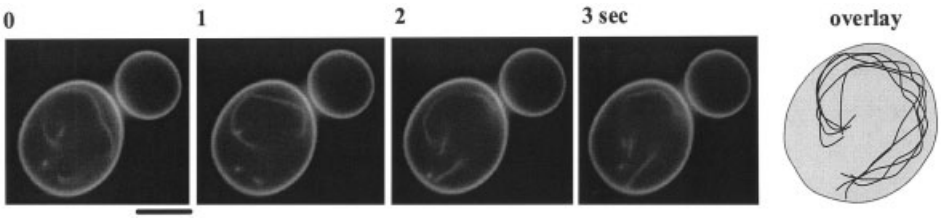

Figure 6. Snapshots of an OE7 wormlike micelle encapsulated in an OE7 bilayer vesicle over a 3-s time interval with worm backbone overlays. Because the w_{EO} of OE7 is close to the vesicle-worm transition, polydispersity of the copolymer tends to drive formation of both structures, leading to suspensions of stable, coexisting assemblies (scale bar is 5 μm).

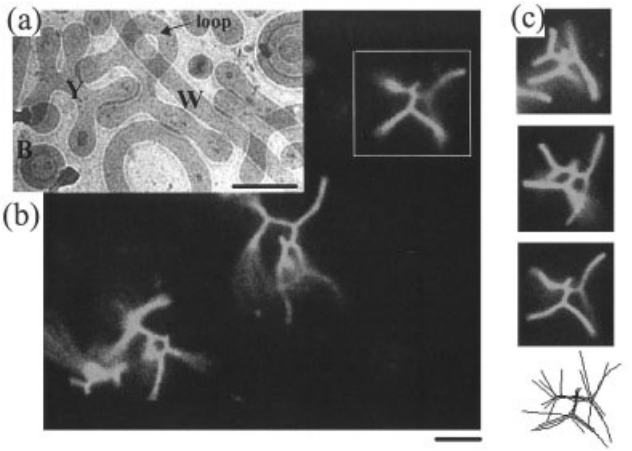

Figure 7. Branched structures form from film hydration of high-molecular-weight OB19 diblock copolymers: (a) cryo-TEM image of various OB19 assemblies adsorbed to a surface where bilayer vesicles (B), Y-junctions (Y), and wormlike micelles (W) are seen in coexistence (scale bar is 0.1 μm); (b) snapshot of fluorescently labeled OB19 branched structures (scale bar is 2 μm); and (c) snapshots and backbone traces of freely diffusing branch indicated in (b), spaced ~2.5 s apart, which show that the arms of the branch bend around a relatively rigid center section.

consistent with the steric stability designed in with the PEO brushes.

The typical structures formed from amphiphiles, based on the size ratio of the hydrophilic to hydrophobic parts, are bilayer vesicles, wormlike micelles, and spheres. However, when the molecular weight of the amphiphiles is increased to >10–15 kg/mol (greater than that of OB18), a new worm-related structure, referred to as Y-junctions, is found.[15] Figure 7(a) displays a cryo-TEM image of several OB19 structures, which include bilayer vesicles (B), wormlike micelles (W), Y-junctions and loops (Y), and spherical micelles (S). Cryo-TEM images also show that cylinders in Y-junction structures have comparable diameters to OB19 wormlike micelles.[15] Much larger, lower-resolution branched structures are observed in fluorescence images of OB19 assemblies [Fig. 7(b)] where their dynamics follow rigid rotation about a center region or trunk [Fig. 7(c)]. In cells, branching of filaments occurs with specific accessory proteins[30] and appears central to dendritic growth processes that drive cells forward in crawling. Although emulating such living polymerization is the next great challenge, there are still many unanswered questions regarding these copolymers.

Branched structures of OB19 tend to dominate in number over simpler wormlike micelles. The branches nonetheless tend to have similar bending rigidities to the worms, consistent with their similar diameters [Fig. 7(a)], but the junctions or branch points themselves seem softer than the branches. Figure 7(c) shows relatively rigid arms rotating and wobbling in Brownian motion. This softness may reflect lateral diffusion of polydisperse copolymers in and around the junction, leading to soft modes that are particularly exaggerated and favored by the high symmetry.

The phase diagram encompassing the copolymers in Table 1 was extended from Jain and Bates[15] and is sketched in Figure 8; here we summarize observations of micro-meter-sized assemblies as a function of copolymer w_{EO} and N_h.[15] In addition to geometries already studied in detail, the diagram shows the recently observed Y-junction phase (Y), which coexists with bilayer vesi-

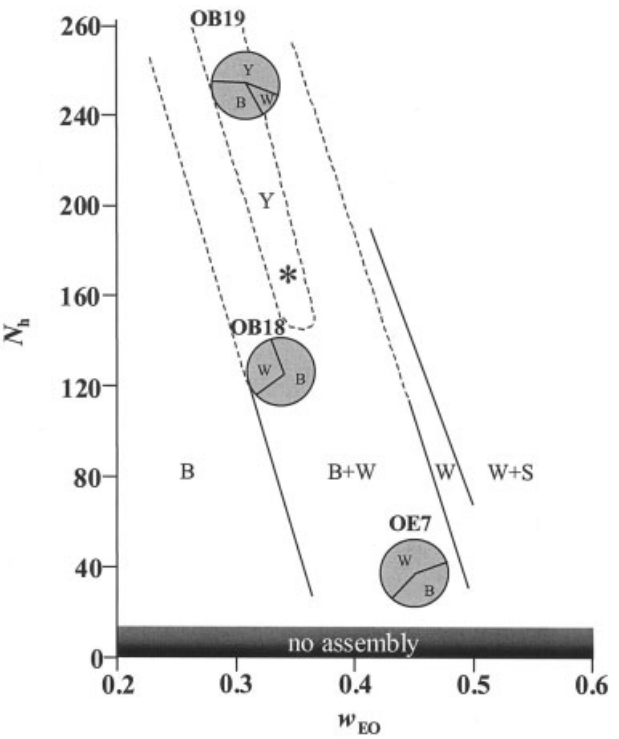

Figure 8. Phase diagram of PEO-PBD/PEE based micro-meter-sized assemblies.[15] Classical phases of bilayer vesicles (B), wormlike micelles (W), and spherical micelles (S) are complimented by a new assembly, Y-junctions (Y), which forms only with high-molecular-weight copolymers and coexists with both vesicles and worms. Pie charts are schematic representations of aggregate mass ratios. The (*) indicates the original Y-former[15] (see Table 1).

cles (B) and wormlike micelles (W) only for the highest molecular weight copolymers.[15] Two copolymers spanning the range were investigated in some detail with respective pie charts indicating the mass-fraction coexistence observable at the micrometer scale. Because we cannot observe sub-micrometer structures, because of optical limitations of fluorescence microscopy, aggregates such as spherical micelles are excluded here. Compared with cryo-TEM, however, the observations here have the advantage of being in water (not frozen) and, more importantly, in thick chambers rather than in the ~100-nm films required for TEM. These results probably provide a better indication of macroscopic stability as opposed to squeezing and fragmentation of soft objects in films.

Issues of stability and bud formation arose in particular with microscopic Y-junction structures given their high curvature and the presence of spherical micelles of comparable diameter [Fig. 7(a)]. From the scaling relationship between l_P and d introduced above, we estimated the persistence length of 8–12 μm for the filaments in the original Y-branches described by Jain and Bates,[15] EO_N-BD_{170} (Table 1) and OB19 here. From the cryo-TEM images in Jain and Bates[15] as well as Figure 7(a), the l_P's allowed us to then calculate a bending free energy (E_{bend}) for loops in Y-junction-dominated structures. Given a typical loop radius of ~100 nm and a persistence length of about 8 μm, we estimated $E_{bend} \sim 100\ \pi k_B T$. Dividing this by the thousands of copolymers comprising the loop makes such a bending energy per molecule only a fraction of $k_B T$ and very small as compared with the energetics holding the aggregates together (e.g., $\alpha > 26\ k_B T$).[7] This tight bending of fluid worms is thus feasible without significant molecular rearrangement[15] necessary to speculate about the formation of macroloops that are energetically easier to make, and their implications for creating synthetic cytoskeletons or other structures have yet to be explored.

CONCLUSIONS

High-molecular-weight copolymers assembled into stable bilayer vesicles, wormlike micelles, spherical micelles, and at high enough molecular weight Y-junctions. Wormlike micelles can emulate the bending rigidity of various ubiquitous biopolymers from intermediate filaments to microtubules through the selection of different-sized copolymers and chemical fixation of unsaturated butadiene bonds. Fluid wormlike micelles of varying diameter followed the stiffness scaling relation $l_P \sim d^{2.8}$, which more closely mimicked the same relation for a fluid aggregate than a solid rod. Upon chemical fixation, a unique spontaneous curvature was locked into each worm's backbone, which is a property exclusive to these micelles. Although simple capillary forces group wormlike micelles into nematic domains, which are structurally similar to actin cytoskeletons, worms can also be encapsulated in bilayer vesicles when the w_{EO} of the copolymer is close to the bilayer/worm transition. Such processes yield all-synthetic mimics of filament-in-lipid bilayer structures typical of cells. Finally, when the molecular weight of the copolymers is increased to >10–15 kg/mol, a new assembly is found, Y-junctions, which exhibit morphology between worms and vesicles.

The authors thank Frank Bates (University of Minnesota) for a careful reading of this article as well as for his group's generous provision of the copolymers and cryo-TEM images. The authors also thank H. Aranda-Espinoza for the valuable discussions. Funding was provided by NSF-MRSEC and the Penn-Drexel Nano-Tech Institute.

REFERENCES AND NOTES

1. Discher, B. M.; Won, Y. Y.; Ege, D. S.; Lee, J. C. M.; Bates, F. S.; Discher, D. E.; Hammer, D. A. Science 1999, 284, 1143.
2. Discher, B. M.; Bermudez, H.; Won, Y.-Y.; Bates, F. S.; Hammer, D. A.; Discher, D. E. J Phys Chem B 2002, 106, 11.
3. Zhang, L. F.; Eisenberg, A. Science 1995, 268, 1728.
4. Cornelissen, J. L. M.; Fischer, M.; Sommerdijk, A. J. M.; Nolte, R. J. M. Science 1998, 280, 1427.
5. Nardin, C.; Hirt, T.; Leukel, J.; Meier, W. Langmuir 2000, 16, 1035.
6. Won, Y. Y.; Davis, H. T.; Bates, F. S. Science 1999, 283, 960.
7. Dalhaimer, P.; Bates, F. S.; Discher, D. E. Manuscript in revision.
8. Fudge, D. S.; Gardner, K. H.; Forsyth, T.; Riekel, C.; Gosline, J. M. Manuscript in preparation.
9. Gittes, F.; Mickey, B.; Nettleton, J.; Howard, J. J Cell Biol 1993, 120, 4.
10. Kas, J.; Strey, H.; Barmann, M.; Sackmann, E. Europhys Lett 1993, 21, 865.
11. Grosberg, A. Y.; Khokhlov, A. R. Statistical Mechanics of Macromolecules; A.I.P.: Woodbury, NY, 1994; Chapter 1.

12. Won, Y. Y.; Paso, K.; Davis, H. T.; Bates, F. S. J Phys Chem B 2001, 105, 8302.
13. Won, Y. Y.; Davis, H. T.; Bates, F. S.; Agamalian, M.; Wignall, G. D. J Phys Chem B 2000, 104, 7134.
14. Won, Y. Y.; Brannan, A. K.; Davis, H. T.; Bates, F. S. J Phys Chem B 2002, 106, 3354.
15. Jain, S.; Bates, F. S. Science 2003, 300, 460.
16. Discher, D. E.; Eisenberg, A. Science 2002, 297, 967.
17. Hillmyer, M. A.; Bates, F. S. Macromolecules 1996, 29, 6994.
18. Bermudez, H.; Brannan, A. K.; Hammer, D. A.; Bates, F. S.; Discher, D. E. Macromolecules 2002, 35, 8203.
19. Bates, F. S.; Fredrickson, G. H. Annu Rev Phys Chem 1990, 41, 525.
20. Bates, F. S. Science 1991, 251, 898.
21. Almdal, K.; Hillmyer, M. A.; Bates, F. S. Macromolecules 2002, 35, 7685.
22. Gestoso, P.; Nicol, E.; Doxastakis, M.; Theodorou, D. N. Macromolecules 2003, 41.
23. Landau, L. D.; Lifshitz, E. M. Theory of Elasticity, 3rd ed.; Butterworth-Heinemann: Oxford, 1986; Chapter 2.
24. Bloom, M.; Evans, E.; Mouritsen, O. G. Q. Rev Biophys 1991, 24, 293.
25. Feng, S.; Sen, P. N. Phys Rev Lett 1984, 52, 3.
26. Lee, J. C.; Santore, M.; Bates, F. S.; Discher, D. E. Macromolecules 2002, 35, 323.
27. Muhammad, S. Applications of Percolation Theory; Taylor & Francis: London, 1994; pp 9–20.
28. Ahmed, F.; Hategan, A.; Discher, D. E.; Discher, B. M. Langmuir, in press.
29. Limozin, L.; Sackmann, E. Phys Rev Lett 2002, 89, 168103.
30. Blanchoin, L.; Amann, K. J.; Higgs, H. N.; Marchand, J.-B.; Kaiser, D. A.; Pollard, T. D. Nature 2000, 404, 1007.